RSC Advances

PAPER

View Article Online
View Journal | View Issue

Cite this: *RSC Adv.*, 2019, **9**, 40222

Synthesis of N-doped carbon dots and application in vanillin detection based on collisional quenching†

Yongping Wang, Qiaoli Yue, * Yingying Hu, Chen Liu, Lixia Tao and Cong Zhang

Received 13th October 2019
Accepted 13th November 2019

DOI: 10.1039/c9ra08352a

rsc.li/rsc-advances

N-doped carbon dots (NCDs) exhibit bright blue emissions and have been used as viable fluorescent probes in the turn-off fluorometric assay for vanillin detection. NCDs were prepared from glucose and tyrosine using a facile and green synthesis process. The one-pot hydrothermal treatment was used without any strong acid or oxidant. The fluorescence of NCDs (with excitation/emission peaks at 323/416 nm, respectively) can be quenched by vanillin. The quenching mechanism belongs to the dynamic quenching mode due to the molecular collisions of the ground state of vanillin and the excited state of NCDs. This turn-off system could be utilized to quantify vanillin within a linear range of 0.43–264 μM. The limit of detection was 0.10 μM. Moreover, this approach was successfully applied toward the determination of vanillin in food samples.

Introduction

Carbon dots (CDs) are a new and promising class of fluorescent carbon nanostructure candidates, which were firstly explored in 2004 during the purification of single-walled carbon nanotubes.[1] CDs exhibit strong and tunable fluorescence properties, high photostability, and unique photoluminescence behaviors.[2,3] By virtue of these distinct optical benefits, CDs show a variety of applications in fluorescent ink,[4] bioimaging,[5] drug delivery[6] as well as sensing.[7–10] However, the relatively low quantum yield (QY) of nonfunctionalized CDs, usually consisting of carbon and oxygen elements, is usually a limiting factor for their wider applications. To improve the QY of CDs, surface modification *via* elemental doping has often been employed.[11–15] Nitrogen (N) is one of the most widely used elements for doping on CD structures. Since N-doped CDs (NCDs) were first reported in the reaction of photoelectrochemical H_2 evolution,[16] various NCD semiconductor hybrids have been prepared and widely used.[17,18] Herein, we synthesized and used NCDs as fluorescence probes for the detection of vanillin (4-hydroxy-3-methoxybenzaldehyde, $C_8H_8O_3$).

Vanillin has the form of white or slightly yellow colored needles or crystalline powder with a sweet, creamy, vanilla odor. Vanillin is mainly used as a flavoring agent, primarily in foods and beverages (such as chocolate and dairy products). It is also used to mask unpleasant tastes in medicines or livestock fodder. Moreover, vanillin has been recognized as an important bioactive compound imparting antioxidant activity[19] and antimicrobial effects in fresh fruit, milk,[20] and synergistic effect.[21] According to the regulations of the U.S. Food and Drug Administration (FDA), the concentration of vanillin in food should not exceed 70 mg kg^{-1}. China's National Food Safety Standard (GB-2760-2011)[21] requires that the amount of vanillin used in the preparation of vanilla, chocolate, or butter should be in the range from 25% to 30% and the amount directly used in biscuits and cakes should be in the range from 0.1% to 0.4%. Furthermore, the usage of vanillin is forbidden in formula for infants less than 6 months due to the potential impairment of liver, kidney, and spleen functions.[22,23] Therefore, the concentration of vanillin should be carefully controlled during food production in addition to considering the potential environmental pollution effects. Several methods have been used to monitor vanillin concentrations. They include high-performance liquid chromatography (HPLC) with or without mass spectrometry (MS),[24] capillary electrophoresis,[25] electrochemistry,[26,27] spectrophotometry,[28] as well as spectrofluorometry.[29] When comparing these methods, the fluorescence method has been considered to be a promising technique due to its potential advantages such as low cost, easy operation, and high sensitivity and selectivity.[30]

In this work, NCDs with bright blue fluorescence have been synthesized using the one-pot hydrothermal method. NCDs have been prepared from glucose and tyrosine without using a strong acid or oxidant. Moreover, the blue emissions from NCDs can be significantly quenched by vanillin, suggesting their potential applications for the detection of vanillin.

Department of Chemistry, Liaocheng University, Liaocheng 252059, China. E-mail: yueqiaoli@yahoo.com

† Electronic supplementary information (ESI) available. See DOI: 10.1039/c9ra08352a

Experimental

Materials and reagents

Glucose, tyrosine, and vanillin were purchased from Sigma-Aldrich (St. Louis, MO, USA). The metal salts were ordered from Aladdin Reagent Co., Ltd. (Shanghai, China). These salts were $Fe(NO_3)_3$, $CuCl_2$, $HgCl_2$, $Co(NO_3)_2 \cdot 6H_2O$, $AgNO_3$, $CaCl_2$, $NiCl_2$, $Mn(CH_3COO)_2$, $MgCl_2$, $CrCl_3$, $Bi(NO_3)_3 \cdot 5H_2O$, and $Pb(NO_3)_2$. Some possible interference species were obtained from Sinopharm Chemical Reagent Co., Ltd. (Shanghai, China). They were bisphenol AP, estradiol, hydroquinone (HQ), resorcinol (RC), pyrocatechol (CC), salicylic acid, PHP, paraben, ninhydrin, anhydrous ethanol, ethyl acetate, and toluene. HEPES, phosphate buffer (PB), tris(hydroxymethyl)aminomethane (Tris), HAc, and NaAc were purchased from Aladdin Reagent Co., Ltd. (Shanghai, China, http://www.aladdin-e.com). They were used for the adjustment of pH. All the chemicals obtained from commercial sources were of the analytical grade and used directly without further purification, unless there were special instructions. All the solutions were prepared and diluted by ultrapure water, which was obtained from a Milli-Q water purification system.

Instruments

Fluorescence spectra and fluorescence intensity were obtained on an F-7000 spectrophotometer (Hitachi, Japan). The absorption spectral measurements were carried out on a Lambda 750 spectrophotometer (PerkinElmer, USA). The transmission electron microscope (TEM) data were performed on a JEM 2100 electron microscope (JEOL Ltd., Japan). TEM worked at an acceleration voltage at 200 kV, and a carbon-coated copper grid was used for sample suspension. The Fourier-transform infrared (FT-IR) spectra were obtained on a Nicolet 6700 FT-IR spectrophotometer (Thermo Scientific Ltd., USA). X-ray photoelectron spectroscopy (XPS) measurements were undertaken with a K-Alpha Spectrometer (Thermo Scientific Ltd., USA). Digital photographs of the CD dispersion under daylight and UV lamp illuminations were captured by a Coolpix 4500 digital camera (Nikon, Japan, https://www.nikon.co.jp).

Preparation of NCDs

The NCDs were synthesized using a Teflon-sealed autoclave reactor in a DZ-2A vacuum drying oven (Tianjin Taisite Instrument Co., Ltd.) by means of a hydrothermal approach. The hydrothermal method has been widely used for CD synthesis.[31–33] Briefly, 0.5 g glucose and 0.5 g tyrosine were firstly dissolved and completely mixed in 6 mL deionized water. The mixture was transferred into a 25 mL Teflon stainless steel autoclave and heated at 180 °C for 9 h. The resultant product was purified in a centrifuge (5000 rpm) for 30 min to remove the agglomerated particles. The supernatant was further dialyzed against deionized water for 24 h to remove the excess reactants. Thereafter, the resulting reddish brown and transparent product was freeze-dried to yield the final NCD powder. The as-prepared NCDs were redispersed in ultrapure water (0.47 mg mL^{-1}) and stored at 4 °C before use.

Determination of vanillin

The detection of vanillin was carried out at room temperature in HEPES buffer where the pH was adjusted to 8.0. In a typical assay, a series of standard stock solutions of vanillin with different concentrations were firstly prepared by dissolving vanillin in deionized water. Subsequently, 10 μL vanillin solution containing 0.5 mg mL^{-1} NCDs was mixed with 5 μL vanillin solution under different concentrations and 5 μL EDTA solution (50 mM). The fluorescence emission spectra were recorded at an excitation wavelength of 323 nm in the presence and absence of vanillin. The maximum wavelength values were selected at 323 and 416 nm for excitation and emission, respectively, to measure the fluorescence intensities under different conditions.

To investigate the selectivity of the NCD products present for the vanillin analysis, parallel experiments were carried out using PHB, estradiol, HQ, CC, RC, BQ, bisphenol AP, salicylic acid, ninhydrin, *p*-bromophenol, and *p*-nitrotoluene in a buffer solution with five times higher concentration than that of vanillin under the same experimental conditions.

Pretreatment of food samples

The proposed method was used for vanillin detection in real samples such as biscuits, yogurts, and essential oils. Before the measurements, the samples were appropriately pretreated. In brief, the food samples were purchased from the local supermarkets (Liaocheng, China). The samples were crushed and dissolved in deionized water before use. Further, filtration was carried out with a 0.22 μm membrane (Millipore) to remove the larger particles before use. Then, 10 μL NCD dispersion was mixed with 5 μL food sample, 5 μL EDTA (50 mM), and 5 μL vanillin solutions at different concentrations. The content of vanillin in the food samples was analyzed using the developed sensing technique, and the recovery efficiency was calculated.

Results and discussion

NCD characterization

The schematic illustration for the synthesis of NCD nanoparticles is shown in Scheme 1. The NCD products were prepared from glucose and tyrosine using a hydrothermal method under heat at 180 °C for 9 h. Under normal light, the aqueous solution appears colorless, whereas under UV light (365 nm), a bright blue emission is observed from the NCD dispersion, as shown in Scheme 1. The relative QY of the NCD

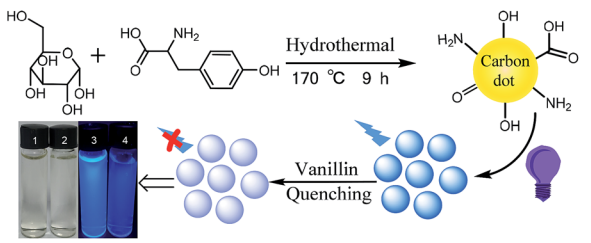

Scheme 1 Schematic of NCD synthesis and application in vanillin detection.

was calculated to be 20.9% using quinine sulphate as the reference (Fig. S1, in the ESI†).

As shown in Fig. 1a, the TEM images reveal that the prepared NCD nanoparticles were spherical and well dispersed without any agglomeration in the aqueous media. The size distribution of the NCDs was estimated to be from 1.48 to 5.12 nm and the average particle diameter was calculated to be 3.03 nm (as shown in the inset of Fig. 1a). Fig. 1b shows an obvious absorption peak at 275 nm and a little shoulder peak at 221 nm in the UV-vis absorption spectrum. The two peaks can be assigned to the conjugation of the n–π* and π–π* transitions of the carbonyl group (C=O) and C=C bonds, respectively.

The surface functionalization of the NCDs was further confirmed by FT-IR analysis. Fig. S2a (in the ESI†) shows the FT-IR spectra of the NCD products. The broad absorption band at 3450 cm^{-1} can be assigned to the stretching vibrations of N–H and O–H. This indicates the abundance of amino and hydroxyl groups on the surface of NCDs, which is beneficial toward the hydrophilic properties of NCDs. The strong absorption at 1635 cm^{-1} can be attributed to the stretching vibrations of C=O or C=N of the amide groups,[30] whereas the peak at 1513 cm^{-1} is due to the O=C–NH_2 or C=C stretching vibrations.[4] The absorption peak at 1234 cm^{-1} can be ascribed to the typical stretching vibration of C–N. It can be initially confirmed that there are C=O, C=N, C=C, C–N and NH_2 groups on the surface of NCDs.

Fig. S2b (in the ESI†) shows the XRD pattern of the NCD products. This suggests that NCDs have an amorphous rather than a crystal structure since there is a broad peak at $2\theta = 22°$.[6]

The XPS analysis was carried out to reveal the extent of N-doping and further characterization of the binding styles of carbon, nitrogen, and oxygen in the NCD nanostructures. The content of nitrogen is about 4.97%, as shown in Fig. S2c (in the ESI†). It reveals that the peaks at about 285.6, 400.5, and 533.0 eV correspond to C 1s, N 1s, and O 1s, respectively. Fig. S2d (in the ESI†) shows the high-resolution C 1s spectrum. There are four peaks at 283.6 (C–O), 284.2 (C=C or C–C), 285.5 (C–N), and 290.7 (R–C=O) eV. Fig. S2e (in the ESI†) shows the high-resolution spectrum of N 1s, which can be deconvoluted into five peaks at 398.8, 399.6, 400.7, 401.5, and 405.3 eV, which can be associated with pyridinic N; N–O or NC–R; graphitic N; –NH_2; and O–N–O bonds, respectively. Fig. S2f (in the ESI†) shows five peaks at 530.7, 531.0, 531.7, 532.5, and 533.1 eV, which can be attributed to the O–H, C–O, C=O, O–C–N, and C–O–C bindings, respectively. Thereafter, the NCD products formed nitrogen-doped amino-dominant carbon quantum dots. The functional groups facilitated the enhancement of the aqueous dispersibility and stability.

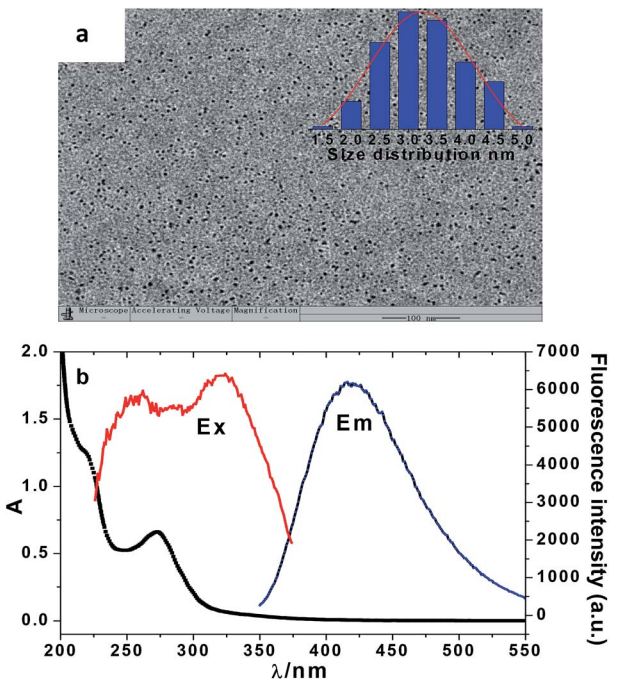

Fig. 1 TEM images. Inset: particle diameter distribution (a) and absorption, excitation, and emission spectra of the NCDs (b).

Optimization of sensing conditions

NCD products were synthesized using a hydrothermal method and used for the determination of vanillin (Scheme 1). The optimal experimental conditions for the synthesis of NCD and sensing of vanillin were investigated. These conditions were molar ratio, reaction time, temperature, and solvent pH for the synthesis process and excitation wavelength, buffer species, pH, and ion strength for the sensing process.

Effect of synthesis conditions. Glucose was often recommended as the raw material for fluorescent and phosphorescent CD preparations.[34] Herein, we initially used glucose and tyrosine as the precursors to synthesize NCD products, where nitrogen was derived from tyrosine. Due to the effect of the levels of nitrogen on the optical properties of NCDs,[35] the molar ratio of glucose and tyrosine was studied, as shown in Fig. S3a (in the ESI†). Evidently, the relative fluorescence intensity of the NCD increases as the molar ratios of glucose and tyrosine increase from 1 : 5 to 1 : 1 and reduce from 1 : 1 to 5 : 1. The fluorescence intensity of the NCD reaches its maximum with the molar ratio of glucose and tyrosine at 1 : 1.

The reaction time and temperature were determined. Fig. S3b (in the ESI†) shows the fluorescence intensity of the NCD with the reaction time ranging from 8 to 12 h. It can be observed that the fluorescence intensity reaches the peak for a reaction time of 9 h. Therefore, 9 h was used as the optimum condition for subsequent experiments. Reaction temperatures ranging from 160 to 200 °C were used for the hydrothermal reaction of glucose and tyrosine. The relative fluorescence intensities of the NCDs were recorded under different reaction temperatures. Evidently, the fluorescence intensity reaches its peak when the reaction was at 180 °C, as shown in Fig. S3c (in the ESI†).

Ultrapure water was used as the solvent for the reaction of glucose and tyrosine. The effect of pH on the reaction system was studied. The fluorescence intensities of the NCD products were measured in aqueous media for different pH values. As shown in Fig. S3d (in the ESI†), the fluorescence intensity of the NCD reaches the maximum at pH 9 within the pH range from 6

to 10. All the measurements were tested three or more times; the relative standard deviation (RSD) was calculated with the error bars, as shown in Fig. S3d (in the ESI†).

Effect of excitation wavelength. Fig. S4a (in the ESI†) shows the fluorescence spectra of the NCD dependence on the excitation wavelength. Evidently, the emission peak is dependent on the excitation wavelength. The emission peak marginally shifts to a longer wavelength with excitation from 290 to 330 nm and the intensity increases, while the peak continues to shift to longer emission wavelengths and the intensity sharply decreases when the excitation varies from 330 to 390 nm. The fluorescence intensity reaches its maximum value (λ_{max}(em) = 416 nm) at an excitation wavelength of 323 nm. This result agrees with that of an earlier report, which may be attributed to the optical selection of the quantum effect with different sized nanoparticles, different emissive traps, and different polyaromatic fluorophores on the structure of the NCD core.[36] Therefore, the fluorescence intensity was recorded with the excitation and emission wavelengths set at 323 and 416 nm, respectively.

Effect of sensing conditions. To determine the optimum sensing conditions for vanillin detection, the effect of buffer species (pH 8.0), pH, and ion strength were investigated. The system solution could be adjusted with different species such as HEPES (8.00), PB (7.96), Tris–HCl (8.04), and HAc–Ac^- (8.05). Fig. S4b (in the ESI†) shows the relative fluorescence intensities of NCD, NCD–vanillin, and vanillin, as well as F_0–F changes with the buffer species. It can be observed that there is almost no change in the fluorescence intensity of NCD and vanillin. The value of F_0–F, however, obviously varies, which can be ascribed to the change in the fluorescence intensity of NCD–vanillin. It can be found that the HEPES buffer exhibits better performance. HEPES was employed for the adjustment of system pH for vanillin determination. The fluorescence intensities for NCD, NCD–vanillin, and vanillin were measured, and F_0–F was calculated under different pH values. As shown in Fig. S4c (in the ESI†), the fluorescence intensity of the NCD is relatively stable within the pH range of 4.0–9.0, and it drops sharply when the pH exceeds 9.0. There is a slight change in the fluorescence intensity of vanillin. With regard to the intensity of NCD–vanillin, there is a peak at pH 4.0. From the F_0–F results, a platform is evident at pH 8.0–10.0. To avoid the additional effect of pH in real samples, pH 8.0 was selected as the optimum condition. Therefore, pH 8.0 in the HEPES buffer was selected for the subsequent experiments. The effect of ion strength on the system's fluorescence was carried out by using NaCl at different concentrations. Fig. S4d (in the ESI†) shows that there is almost no obvious change in the fluorescence intensity of the NCD with a series of NaCl solutions. It can be deduced that there is almost no influence of ion strength on the system's fluorescence.

Sensitivity

Before performing the sensitivity measurements, the fluorescence and absorption spectra of the NCDs were investigated in the presence and absence of vanillin. Fig. 2a and b show the fluorescence and absorption spectra of NCD, vanillin, and NCD–vanillin, respectively. The fluorescence intensity of NCD is obviously strong and vanillin shows weak fluorescence. After the addition of vanillin, the fluorescence of NCD was significantly quenched. By comparison, the absorption spectrum of NCD–vanillin can be attributed to the superimposition of the spectra from both NCD and vanillin (Fig. 2b). It can be deduced that there is almost no new formation of complexes between NCD and vanillin.

The sensitivity toward vanillin detection was investigated under optimum experimental conditions. They include precursor materials ratio of 1 : 1, reaction time of 9 h under 180 °C, in aqueous media at pH 9.0, excitation wavelength at 323 nm, and pH 8.0 adjusted by the HEPES buffer. As shown in Fig. 2c, the fluorescence intensity of NCD regularly varied with different concentrations of vanillin (0, 0.4, 1, 2, 4, 10, 20, 40, 100, 200, and 264 μM). This clearly demonstrates that the fluorescence of NCDs can be gradually quenched by vanillin with an increase in concentration. Fig. 2d shows that F_0–F exhibits a good linear relationship (R^2 = 0.9972) *versus* the concentration of vanillin (ranging from 0.43 to 264 μM). The fluorescence intensity was recorded at 416 nm. The limit of detection (LOD) was estimated to be 0.10 μM using the equation 3.29 S_B/m according to the IUPAC recommendation. Here, S_B and m denote the standard deviation of the blank (n = 11) and the slope of the calibration graph, respectively. This indicates that NCDs as fluorescence probes can be applied as an efficient sensing method for vanillin detection.

Selectivity

Specificity is an important characteristic for the evaluation of the capability of a system. Firstly, some metal ions were tested, as shown in Fig. S5a (in the ESI†). It can be observed that some common metal ions such as Ba^{2+}, Bi^{3+}, Hg^{2+}, and particularly Fe^{3+} can also quench the fluorescence of NCDs. To avoid the influence of such metal ions, a masking agent, namely,

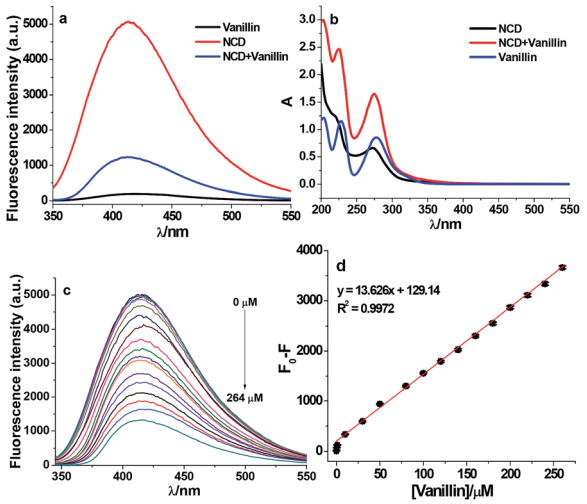

Fig. 2 Fluorescence (a) and absorption (b) spectra of NCDs with and without vanillin, quenching effect of vanillin on the fluorescence spectra of NCDs (c), and the linear response of fluorescence change (F_0–F) on the concentration of vanillin (d). The error bars show the average of three separate measurements (d).

ethylenediaminetetraacetic acid disodium salt (EDTA), was added to the detection system. As shown in Fig. S5b (in the ESI†), the fluorescence of NCDs is not affected by all the metal ions tested in the presence of EDTA–2Na.

The influence of certain possible interfering organic molecules with structures similar to vanillin was also investigated. These species include PHB, estradiol, HQ, CC, RC, BQ, bisphenol AP, salicylic acid, ninhydrin, *p*-bromophenol, and *p*-nitrotoluene. As shown in Fig. 3, only vanillin (200 μM) could significantly quench the fluorescence of NCDs; the other molecules at higher concentrations (1 mM) could not affect the intensity. This indicates that the detection strategy exhibits a specific fluorescence response toward vanillin for the common organic molecules with similar structures. This also suggests that the developed assay can provide good specificity toward monitoring vanillin in the samples with similar structures.

Possible fluorescence quenching mechanism

When a molecule is electronically excited by the absorption of a photon, the species can return to the ground state *via* several avenues. One of them involves the emission of a photon, which can cause the substance to fluorescence or phosphorescence. There are two modes, however, where there are collisions or complexes formation between the excited molecules and other atoms or molecules. Nonradiative schemes are called dynamic or collisional quenching and static quenching. With regard to dynamic quenching, the quencher must diffuse into the fluorophore during the lifetime of the excited state, without emitting a photon. The collisional quenching of fluorescence is described by the Stern–Volmer equation:

$$\frac{F_0}{F} = 1 + k_q\tau_0[Q] = 1 + K_D[Q] \quad (1)$$

In this equation, F_0 and F denote the fluorescence intensity in the absence and presence of a quencher, respectively; k_q is the bimolecular quenching constant; τ_0 is the lifetime of the fluorophore without a quencher; and [Q] is the concentration of the quencher. Further, K_D represents the Stern–Volmer constant, expressed as $K_D = k_q\tau_0$, when the quenching is dynamic. Otherwise, this constant can be described as K_{sv} for

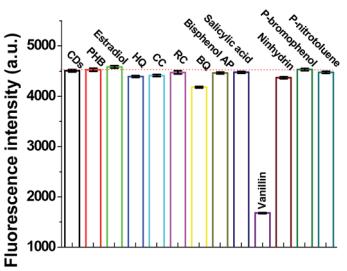

Fig. 3 Selectivity test for the determination of vanillin in the presence of other organic molecules with structures similar to that of vanillin. The error bars denoted three separate measurements with RSD less than 1.0% (concentrations: NCD: 0.47 mg mL^{-1}; vanillin: 200 μM; other species: 1 mM).

Table 1 Determination of vanillin in food samples[a]

Sample	Added μM	Found μM	Recovery%	RSD%
Biscuits	0.0	0.50	—	2.13
	5.0	5.44	98.7	0.74
	10.0	10.23	97.2	1.09
Yogurt	0.0	0.48	—	3.02
	5.0	5.57	101.6	1.07
	10.0	10.36	98.9	2.21
Essential oil	0.0	2.93	—	1.89
	5.0	7.80	97.2	3.05
	10.0	13.40	105.1	1.28

[a] Mean of three separate measurements.

the static quenching mode. From Fig. S6a (in the ESI†), it can be observed that the Stern–Volmer plot has an upward curvature and forms a concave shape toward the *y*-axis. This characteristic feature is due to both collisions and complex formation. Since a higher temperature can result in faster diffusion and hence larger amounts of collisional quenching, the two modes can be distinguished by their differing dependences on temperature. Fig. S6b (in the ESI†) shows that the slope values of the plots increase with the temperature. This suggests that fluorescence quenching may be mainly ascribed to collisional contact. In addition, to further confirm the quenching mode of vanillin for the fluorescence of NCDs, the lifetime was investigated. From the fluorescence decay curves (Fig. S6c, in the ESI†), it can be found that the lifetimes were calculated to be 7.65 and 6.00 μs for NCDs in the absence and presence of vanillin, respectively. The decrease in lifetime occurs because quenching is an additional rate process that depopulates the excited state without any fluorescence emission. It can be deduced that fluorescence quenching is because of the dynamic mode since static quenching does not decrease the lifetime. The dynamic quenching constant k_q was also obtained (Table S1†) using the slope of the Stern–Volmer plot and the lifetime of NCDs without vanillin according to eqn (1). Evidently, all the values of k_q are 108 L mol^{-1} s^{-1} and they increase with the temperature (from 5 to 45 °C). The values of k_q are smaller than the diffusion-controlled value (1010 L mol^{-1} s^{-1}), which can result from the steric shielding of the fluorophore or low quenching efficiency. For the fluorophores, this occasionally allows selective quenching. The occurrence of quenching depends upon the mechanism, which, in turn, depends on the chemical properties of the individual molecules. A further detailed analysis of the mechanism of quenching is complex.

Application

The practical applications of NCD fluorescence probes for vanillin determination in foodstuff (biscuits, yogurts, and essential oils) were carried out. The results for the content of vanillin, recovery, and RSD are listed in Table 1. The results of the recovery and RSD reveal that the proposed method exhibits acceptable precision and accuracy. The NCD products applied as fluorescence probes can be used for the detection of vanillin

in certain common food samples. Therefore, the accuracy of the proposed method is acceptable and may be preliminarily applied for monitoring vanillin in complex samples.

Conclusions

In summary, a turn-off fluorescence approach for vanillin detection was formulated based on the fluorescence quenching of vanillin on the bright blue emissions of NCDs. NCDs were synthesized *via* a one-pot hydrothermal reaction using glucose and tyrosine as the precursor materials. NCDs show a QY of 20.9%. Vanillin can significantly quench the fluorescence of NCDs. The possible quenching mode can be mainly ascribed to the dynamic quenching mode resulting from the molecular collisions between the excited state of NCDs and the ground state of vanillin. The decrease in the fluorescence intensity was in proportion to the concentration of vanillin. When NCDs are used as a fluorescence probe, the system displays high specificity toward vanillin detection even in the presence of other organic molecules with similar structures. The developed fluorescence approach was successfully applied for the determination of vanillin in aqueous media, as well as in a practical complex matrix of food samples. It can be deduced that the proposed NCD products can be exploited for the detection of vanillin in more foodstuff or environmental applications.

Conflicts of interest

There are no conflicts to declare.

Acknowledgements

This work was supported financially by Natural Science Foundation of China (91543206), Natural Science Foundation (ZR2014BQ017, ZR2015BM024, and 2013SJGZ07) and Tai-Shan Scholar Research Fund of Shandong Province and research foundation of Liaocheng University.

Notes and references

1 X. Y. Xu, R. Ray, Y. L. Gu, H. J. Ploehn, L. Gearheart, K. Raker, *et al.*, *J. Am. Chem. Soc.*, 2004, **126**, 12736–12737.
2 L. Yan, Y. Yang, C. Q. Ma, X. Liu, H. Wang and B. Xu, *Carbon*, 2016, **109**, 598–607.
3 T. Y. Juang, J. C. Kao, J. C. Wang, S. Y. Hsu and C. P. Chen, *Adv. Mater. Interfaces*, 2018, **5**, 1800031.
4 S. R. Anand, A. Bhati, D. Saini, C. N. Gunture, N. Chauhan, P. Khare, *et al.*, *ACS Omega*, 2019, **4**, 1581–1591.
5 P. Khare, A. Bhati, S. R. Anand, C. N. Gunture and S. K. Sonkar, *ACS Omega*, 2018, **3**, 5187–5194.
6 M. Sabet and K. Mahdavi, *Appl. Surf. Sci.*, 2019, **463**, 283–291.
7 D. Chakraborty, S. Sarkar and P. K. Das, *ACS Sustainable Chem. Eng.*, 2018, **6**, 4661–4670.
8 X. C. Sun and Y. Lei, *Trends Anal. Chem.*, 2017, **89**, 163–180.
9 N. Vasimalai, V. Vilas-Boas, J. Gallo, M. de F. Cerqueira, M. Menéndez-Miranda, J. M. Costa-Fernández, *et al.*, *Beilstein J. Nanotechnol.*, 2018, **9**, 530–544.
10 F. X. Wang, Z. Y. Gu, W. Lei, W. J. Wang, X. F. Xia and Q. L. Hao, *Sens. Actuators, B*, 2014, **190**, 516–522.
11 P. W. Gong, L. Sun, F. Wang, X. C. Liu, Z. Q. Yan, M. Z. Wang, *et al.*, *Chem. Eng. J.*, 2019, **18**, 31813–31818.
12 X. W. Wang, G. Z. Sun, P. Routh, D.-H. Kim, W. Huang and P. Chen, *Chem. Soc. Rev.*, 2014, **43**, 7067–7098.
13 Y. Park, J. Yoo, B. Lim, W. Kwon and S.-W. Rhee, *J. Mater. Chem. A*, 2016, **4**, 11582–11603.
14 S. Y. Liu, N. Zhao, Z. Cheng and H. G. Liu, *Nanoscale*, 2015, **7**, 6836–6842.
15 P. F. Shen and Y. S. Xia, *Anal. Chem.*, 2014, **86**, 5323–5329.
16 Z. L. Wu, Z. X. Liu and Y. H. Yuan, *J. Mater. Chem. B*, 2017, **5**, 3794–3809.
17 W. L. Gao, Y. M. Ma, Y. M. Zhou, H. Song, L. Li, S. H. Liu, X. Q. Liu, B. Gao, C. Z. Liu and K. P. Zhang, *Mater. Lett.*, 2018, **216**, 84–87.
18 Y. P. Wang, Q. L. Yue, L. X. Tao, C. Zhang and C.-Z. Li, *Microchim. Acta*, 2018, **185**, 550.
19 I. Mourtzinos, S. Konteles, N. Kalogeropoulos and V. T. Karathanos, *Food Chem.*, 2009, **114**, 791–797.
20 S. Durant and P. Karran, *Nucleic Acids Res.*, 2003, **31**, 5501–5512.
21 H. L. Wang, J. Y. Zhang and J. B. Zhang, *Chinese Journal of Food Hygiene*, 2011, **23**, 571–575.
22 P. H. Deng, Z. F. Xu, R. Y. Zeng and C. X. Ding, *Food Chem.*, 2015, **180**, 156–163.
23 L. Shang, F. Q. Zhao and B. Z. Zeng, *Food Chem.*, 2014, **151**, 53–57.
24 M. Bononi, G. Quaglia and F. Tateo, *J. Agric. Food Chem.*, 2015, **63**, 4777–4781.
25 S. Minematsu, G. S. Xuan and X. Z. Wu, *J. Environ. Sci.*, 2013, **25**, S8–S14.
26 Q. W. Mei, Y. P. Ding, L. Li, A. Q. Wang, D. D. Duan and Y. J. Zhao, *J. Electroanal. Chem.*, 2019, **833**, 297–303.
27 L. Jiang, Y. P. Ding, F. Jiang, L. Li and F. Mo, *Anal. Chim. Acta*, 2014, **833**, 22–28.
28 J. Zhao, H. X. Xia, T. Y. Yu, L. Jin, X. H. Li, Y. H. Zhang, L. P. Shu, L. W. Zeng and Z. X. He, *PLoS One*, 2018, **13**, e0194010.
29 L. Li, Q. L. Zhang, Y. P. Ding, Y. X. Lu, X. Y. Cai and L. R. Yu, *J. Fluoresc.*, 2015, **25**, 897–905.
30 M. C. Rong, Y. F. Feng, Y. R. Wang and X. Che, *Sens. Actuators, B*, 2017, **245**, 868–874.
31 C. L. Xia, S. J. Zhu, T. L. Feng, M. X. Yang and B. Yang, *Adv. Sci.*, 2019, 190131.
32 D. Xu, Q. L. Lin and H.-T. Chang, *Small Methods*, 2019, 1900387.
33 B. B. Chen, M. L. Liu, C. M. Li and C. Z. Huang, *Interface Sci.*, 2019, **270**, 165–190.
34 P. Long, Y. Y. Feng, C. Cao, Y. Li, J. K. Han, *et al.*, *Adv. Funct. Mater.*, 2018, **28**, 1800791.
35 Y. Xiong, J. Schneider, C. Reckmeier, H. Huang, P. Kasak and A. Rogach, *Nanoscale*, 2017, **9**, 11730–11738.
36 J. L. Ci, Y. Tian, S. Kuga, Z. W. Niu, M. Wu and Y. Huang, *Chem.–Asian J.*, 2017, **12**, 2916–2921.